Published in final edited form as:
J Invest Dermatol. 2012 June ; 132(6): 1543–1553. doi:10.1038/jid.2012.27.

The cell-cycle regulator protein 14-3-3σ is essential for hair follicle integrity and epidermal homeostasis

Nigel L. Hammond[1], **Denis J. Headon**[2], and **Michael J. Dixon**[1]

[1]Faculty of Medical and Human Science and Faculty of Life Sciences, Manchester Academic Health Sciences Centre, University of Manchester, Oxford Road, Manchester M13 9PT

[2]The Roslin Institute and Royal (Dick) School of Veterinary Studies, University of Edinburgh, Roslin, Midlothian, EH25 9PS

Abstract

14-3-3σ (Stratifin; *Sfn*) is a cell cycle regulator intimately involved in the programme of epithelial keratinisation. 14-3-3σ is unique in that it is expressed primarily in epithelial cells and is frequently silenced in epithelial cancers. Despite its well-documented role as a cell cycle regulator and as a tumour suppressor, 14-3-3σ's function in the intricate balance of proliferation and differentiation in epithelial development is poorly understood. A mutation in 14-3-3σ was found to be responsible for the *repeated epilation* (*Er*) phenotype. It has previously been shown $Sfn^{+/Er}$ mice are characterised by repeated hair loss and re-growth while $Sfn^{Er/Er}$ mice die at birth displaying severe oral fusions and limb abnormalities as a result of defects in keratinising epithelia. Here we show mice heterozygous for the 14-3-3σ mutation have severe defects in hair shaft differentiation, resulting in destruction of the hair shaft during morphogenesis. Further, we report the inter-follicular epidermis and sebaceous glands are hyperproliferative, coincident with expanded nuclear Yap1; a critical modulator of epidermal stem cell proliferation. We also report hair follicle stem cells in the bulge cycle abnormally raising important questions as to the role of 14-3-3σ in the bulge.

Introduction

The hair follicle (HF) is a complex mini-organ capable of cyclic regression and regeneration (Stenn and Paus, 2001). During embryogenesis, HF morphogenesis occurs through reciprocal interactions between epithelial and mesenchymal components of the skin, giving rise to eight distinct cell layers of the HF (Hardy, 1992; Millar, 2002; Shimomura and Christiano, 2010). Each HF undergoes periods of growth (anagen), apoptosis-driven regression (catagen) and relative quiescence (telogen) followed by a hair-shedding phase (exogen) (Stenn and Paus, 2001; Milner *et al.*, 2002; Stenn, 2005; Higgins *et al.*, 2009). This capacity for regeneration is maintained by a slowly cycling stem cell (SC) population located in the bulge region of the HF (Cotsarelis *et al.*, 1990; Taylor *et al.*, 2000; Jaks *et al.*, 2010). Recently, other active SC niches have also been discovered within the HF (Nijhof *et al.*, 2006; Horsley *et al.*, 2006; Jaks *et al.*, 2008; Jensen *et al.*, 2009; Snippert *et al.*, 2010).

Inter-follicular epidermis (IFE) is also capable of continuous renewal and harbours a population of mitotically-active cells in the innermost basal layer (Ghazizadeh and Taichman, 2001). These cells divide asymmetrically producing a daughter cell and a transit-

Correspondence: Michael J. Dixon, Faculty of Medical and Human Sciences, Manchester Academic Health Sciences Centre, University of Manchester, Oxford Road, Manchester M13 9PT. Phone: +44-161 275 5620; mike.dixon@manchester.ac.uk.

Conflict of interest The authors state no conflict of interest.

Europe PMC Funders Author Manuscripts

amplifying cell which leaves the basal layer and enters a terminal differentiation program to produce a stratified epidermis (Watt and Hogan, 2000; Blanpain and Fuchs, 2006).

Studies utilising mutant mice have been instrumental in understanding the genes involved in skin and HF biology. The *repeated epilation* (*Er*) mouse mutation has been identified as a single nucleotide insertion in the gene encoding 14-3-3σ (Stratifin) resulting in a truncated protein, thought to act in a dominant negative manner (Herron *et al.*, 2005; Li *et al.*, 2005; Xin *et al.*, 2010a). Homozygous $Sfn^{Er/Er}$ mice die at birth from acute respiratory stress and are characterised by a hyperproliferative epidermis which fails to undergo terminal differentiation (Guenet *et al.*, 1979; Fisher *et al.*, 1987; Herron *et al.*, 2005; Li *et al.*, 2005). Mice heterozygous for the mutation ($Sfn^{+/Er}$) express full-length and truncated forms of 14-3-3σ (Herron *et al.*, 2005; Li *et al.*, 2005), are viable and fertile but show repeated hair loss and re-growth.

14-3-3σ is a member of the 14-3-3 gene family and is involved in fundamental cell functions including cell cycle progression, apoptosis, cell proliferation and differentiation (Aitken, 2006; Medina *et al.*, 2007; Morrison, 2009). 14-3-3σ is expressed exclusively in keratinocytes and is induced during the exit of keratinocytes from the SC compartment (Dellambra *et al.*, 2000; Pellegrini *et al.*, 2001).

While the epidermal proliferation and differentiation defects observed in $Sfn^{Er/Er}$ mice have highlighted the role of 14-3-3σ in epidermal development, the causes of repeated hair loss and re-growth in $Sfn^{+/Er}$ mice are less well understood. Recently, Xin and colleagues suggested hair loss in $Sfn^{+/Er}$ mice results from alterations in club hair anchorage, causing the hair to fall out prematurely (Xin *et al.*, 2010b). Here we report the expression of 14-3-3σ during HF morphogenesis and cycling, and show major HF structural defects in $Sfn^{+/Er}$ mice which result in destruction of the hair shaft and the repeated hair loss and re-growth phenotype. We further report IFE and SG homeostasis is affected in $Sfn^{+/Er}$ mice, displaying a thickened, hyperproliferative epidermis and enlarged SGs. Yes-associated protein 1 (Yap1) has recently been implicated as an essential regulator of epidermal maintenance and SC proliferative capacity, with 14-3-3σ and α-catenin critical modulators in this pathway (Zhang *et al.*, 2011; Schlegelmilch *et al.*, 2011; Silvis *et al.*, 2011). In $Sfn^{+/Er}$ mice we show nuclear Yap1 is increased in thickened, hyperproliferative epidermis. We also report the SC niche in the HF bulge cycles abnormally, raising important questions as to the role of 14-3-3σ in the bulge.

Results

14-3-3σ expression during hair morphogenesis and cycling

14-3-3σ expression was reduced in the epithelial placode (stage 1) compared to surrounding basal epidermis (Figure 1a). The hair germ and peg (stage 2/3) structures were devoid of 14-3-3σ (Figure 1b,c) with expression first seen in the developing inner root sheath (IRS) cone (stage 4) (Figure 1d). The terminally differentiating hair shaft layers (cuticle, cortex and medulla) and companion layer were all positive for 14-3-3σ by stage 8 (Figure 1f).

During catagen, 14-3-3σ was strongly expressed in the germ capsule and epithelial strand of the regressing HF (Figure 1g). 14-3-3σ expression was also observed in companion layer cells surrounding the club hair during telogen (Figure 1h). During first anagen, 14-3-3σ was observed in the IRS cone (anagen IIIa) and later differentiating companion layer and hair shaft components (Figure 1i,j).Cellular localisation of 14-3-3σ within the HF was confirmed by double immunolabelling (Figure S1a-h).

Sfn$^{+/Er}$ mice develop cyclic alopecia

Heterozygous *Sfn*$^{+/Er}$ mice were indistinguishable from wild-type littermates (Figure 2a) until postnatal day (P) 5 when shortened or absent vibrissae were observed on the mystacial pad (Figure S2a,b). The pelage hair phenotype was observed from P7 where areas of apparent hair loss were seen on head and neck regions (Figure 2a; P7). By P10 differences in coat hue were apparent and hair loss had advanced (Figure 2a; P10). Severely affected *Sfn*$^{+/Er}$ mice lost the majority of the first pelage coat by telogen (Figure 2a; P20). New pelage emerged at P28-30 and was progressively lost again (Figure 2a; P30), recapitulating the phenotype seen during HF morphogenesis. *Sfn*$^{+/Er}$ mice failed to re-grow a full coat over subsequent cycles with 6+ month old mice showing permanent patchy alopecia (Figure S2c,d).

Abnormalities in hair shaft differentiation results in hair loss

Histology of P5 backskin revealed normal differentiation of HFs with no obvious defects (Figure 2b). However, at P7 it was evident some HFs had a twisted, irregular appearance (Figure 2c). As morphogenesis proceeded (P10-15), more severely affected HFs were identified with abnormalities of the hair shaft and associated layers (Figure 2d,e). Catagen initiated in a timely manner in most HFs in *Sfn*$^{+/Er}$ mice (P14-P18). The epidermis was noticeably thicker in *Sfn*$^{+/Er}$ mice during catagen and showed hyperkeratosis (Figure 2e), whilst SGs appeared hyperplastic (Figure 2d-f). Staining with Oil Red O revealed increased lipid on the *Sfn*$^{+/Er}$ skin surface and within SGs at P7 (Figure S3a,b). However, at P20 lipid staining was substantially increased in *Sfn*$^{+/Er}$ mice (Figure S3c,d). Severely affected HFs were replaced by keratin-filled cysts that persisted deep in the sub-cutis with most missing a club hair by telogen (Figure 2f). The first adult anagen initiated around P22 with hair re-growth and subsequent loss from P28 onwards (Figure 2g). This mirrored the hair loss from P7 during morphogenesis.

Further analysis of hair shaft formation during morphogenesis (P7-P15) revealed the differentiation of cells of the hair shaft and IRS were disrupted. In these HFs, the path of the emerging hair shaft and IRS was compromised, causing blockages to the HF (Figure 3a,b). Less severely affected HFs were able to produce a hair shaft but abnormalities in septation of the medulla, melanin incorporation and thickness of the hair shaft were seen (Figure 3a). In severely affected HFs, the companion layer, IRS and hair shaft were thickened, showed abnormal cell-cell spaces between layers and were highly eosinophilic, suggesting abnormal differentiation/keratinisation (Figure 3b). Scanning electron microscope (SEM) preparations of skin from affected areas demonstrated the sparseness of emerging hairs during morphogenesis. Analysis of individual hairs from follicles that managed to produce and retain a hair shaft showed striking defects in their cuticular scales, with *Sfn*$^{+/Er}$ mice scales lacking the characteristic ridged pattern (Figure 3c).

Molecular marker analysis of HF defects using dual immunofluorescence for the hair cortex (AE13) and ORS (K5), demonstrated the hair cortex and IRS (unlabelled) were either absent or malformed in the infundibulum of affected *Sfn*$^{+/Er}$ HFs (Figure S4a). AE13 expression in affected HFs demonstrated the irregular morphology of the hair cortex, whilst IRS layers were also thicker and disorganised (Figure S4b). β-catenin signalling is fundamental during HF development, and expression was analysed during HF morphogenesis using total β-catenin and nuclear β-catenin antibodies. Although β-catenin expression appeared normal in the matrix, both antibodies revealed loss of nuclear and cytoplasmic β-catenin in the hair cortex and IRS layers in regions of HF dystrophy (Figure S5a,b; arrows). Our results imply the lack of a club hair is due to defects in hair differentiation, initially within the precortex, affecting the hair cortex and IRS layers, and resulting in an inability to form a proper hair shaft and hence lack of club hair.

Analysis of the interfollicular epidermis

To dissect the skin phenotype further we analysed the IFE at the onset of hair loss (P7) and the stage at which hair loss was most advanced during telogen (P20) using immunofluorescence. The basal cell markers p63 and keratin 14 (K14) showed isolated areas of expansion out of the basal layer epidermis in P7 *Sfn*$^{+/Er}$ mice, this being more pronounced at P20 (Figure 4a-h). The spinous layer marker, keratin 1 (K1), showed expression in the IFE comparable to wild-type at P7 but was also expanded at P20 (Figure 4g,h). Dual immunofluorescence for K14 and K1 showed a subset of the IFE co-expressed both markers in *Sfn*$^{+/Er}$ epidermis at P20 (Figure 4e-h). As these observations suggested the epidermis was hyperproliferative the marker keratin 6 (K6a) was used. K6a is normally absent from stratified epidermis, being restricted to the HF companion layer. However, patchy mis-expression was seen in *Sfn*$^{+/Er}$ epidermis at P7, with expression mainly limited to follicular orifices (Figure 4i,j). By P20, K6a mis-expression was widespread in the IFE (Figure 4k,l). Markers of late-stage epidermal differentiation, such as loricrin and filaggrin, showed expression comparable to wild-type mice at both ages (Figure 4m-p and data not shown).

To further characterise the hyperproliferative IFE, epidermal thickness was measured. At P7, the IFE of *Sfn*$^{+/Er}$ mice was significantly thicker than wild-type littermates (*Sfn*$^{+/Er}$: 29 μm; wild-type: 22 μm: p=0.05), the difference again becoming more pronounced by P20 (*Sfn*$^{+/Er}$: 29 μm; wild-type: 9 μm: p=0.05) (Figure 5a,c-f). BrdU incorporation assays performed at P7 in *Sfn*$^{+/Er}$ mice showed significantly more proliferating basal IFE cells compared to wild-type littermates (*Sfn*$^{+/Er}$: 18%; wild-type: 13%; p=0.05), this difference becoming more pronounced by P20 (*Sfn*$^{+/Er}$: 20%; wild-type: 3%; p=0.05) (Figure 5b,g-j).

Analysis of the transcription factor Yap1, recently linked to 14-3-3σ and implicated in epidermal proliferation and SC maintenance, showed comparable nuclear expression at P7 (Figure 5k,l). However, at P20 expression of nuclear Yap1 was increased in the IFE of *Sfn*$^{+/Er}$ mice compared to wild-type (Figure 5m,n). Dual immunofluorescence for Yap1 and K14 showed a high proportion of Yap1 expressing cells were in expanded basal cells, however Yap1 was expressed throughout the IFE (Figure 5o-r). Expression of α-catenin, another mediator of Yap1 signalling (Schlegelmilch *et al.*, 2011; Silvis *et al.*, 2011), showed no difference at both P7 and P20 ages (Figure 5s-v) and this was reflected by real-time qPCR data at P20 (Figure 5w). Western blot analysis confirmed increased Yap1 protein (70-kDa) in *Sfn*$^{+/Er}$ skin extracts at both P7 and P20. Interestingly, *Sfn*$^{+/Er}$ skin extracts showed smaller doublet bands (43 and 50-kDa) which were always absent from wild-type samples (Figure 5d). Given that α-catenin levels were unchanged, elevated nuclear Yap1 correlated with a thicker, hyperproliferative IFE and this is consistent with Yap1 promoting proliferation and expansion of epidermal progenitors (Camargo *et al.*, 2007; Schlegelmilch *et al.*, 2011; Silvis *et al.*, 2011).

Depletion of label-retaining cells in the hair follicle bulge

Given the cyclic alopecia, hyperplastic SGs and hyperproliferative IFE observed in *Sfn*$^{+/Er}$ mice, we investigated the activity of slowly cycling HF-SCs that reside in the bulge, using a well-characterised BrdU label-retaining cell assay (Figure 6a). Skin samples were taken at P13, 1 day after the last BrdU injection to assess the extent of BrdU incorporation. Immunofluorescence analysis confirmed comparable levels of BrdU labelling between wild-type and *Sfn*$^{+/Er}$ mice (Figure S6a,b). After a 70 day chase (P82), wild-type HFs were in telogen (Figure S6c) and showed numerous BrdU-positive cells (~5-10 per HF) located around the first club hair in the K15-positive bulge (Figure 6b,d,e). In contrast, K15-positive cells in the HF bulge of *Sfn*$^{+/Er}$ littermates were devoid of BrdU label-retaining cells (Figure 6c,f,g) and not all HFs were in telogen, suggesting cycling was also affected (Figure S6d3).

Other markers of HF bulge SCs, such as Sox9 and CD34 were present and appeared expanded (Figure 6h-k). Occasionally small traces of BrdU label were seen in K15-positive bulge cells (Figure 6g). We also investigated possible bulge cell recruitment to SGs and IFE by crossing mice *Krt15*-crePR1 (Ito *et al.*, 2005), R26R and *Sfn*$^{+/Er}$ mice. We found no contribution to either compartment (data not shown). Taken together, these observations are consistent with label being diluted over repeated cell cycles and indicate a cycling defect which may have expanded the stem cell niche of affected *Sfn*$^{+/Er}$ HFs.

Discussion

It has previously been shown in *Sfn*$^{Er/Er}$ mice that 14-3-3σ is a crucial regulator of epidermal homeostasis (Herron *et al.*, 2005; Li *et al.*, 2005). In this study, we investigated the role 14-3-3σ plays in the repeated hair loss and re-growth phenotype seen in *Sfn*$^{+/Er}$ mice.

Initially we investigated the spatio-temporal expression pattern of 14-3-3σ during HF morphogenesis and cycling in wild-type mice (Figure 1), demonstrating that expression of 14-3-3σ coincided with the commitment of cells to differentiate. A similar pattern was seen in the IFE, where expression of 14-3-3σ increased in suprabasal cell layers. In the HF, 14-3-3σ was expressed strongly in differentiating hair shaft layers (medulla, cortex and cuticle) (Figure S1) and defects in these layers appear critical to the complete degeneration of the hair shaft (Ma *et al.*, 2003; Owens *et al.*, 2008; Cai *et al.*, 2009; Kiso *et al.*, 2009). Furthermore, abnormalities in other 14-3-3σ-expressing cells, such as the companion layer, also result in defects in hair shaft production (McGowan *et al.*, 2002).

Xin and colleagues recently attributed hair loss in *Sfn*$^{+/Er}$ mice to alterations in club hair formation, more specifically to companion layer cells which integrate with the club hair during late catagen/telogen (Xin *et al.*, 2010b). In agreement with this study, we observed alterations in the histology of some club hairs which were retained in *Sfn*$^{+/Er}$ mice; however owing to precortex defects we observed during hair follicle morphogenesis (Figures 3, S4, S5) and anagen of the adult cycle, we attribute the majority of hair loss to defects in production of the hair shaft and IRS layers, which as a consequence contributed to the loss of club hairs if any were able to form. Given the expression pattern of 14-3-3σ in HFs and its association with differentiation, we speculate that the transit-amplifying cells within the precortex fail to differentiate in a timely manner, leading to degeneration of the hair shaft and IRS layers.

We have further shown that *Sfn*$^{+/Er}$ mice have defects in IFE homeostasis (Figure 4). The basal cell marker p63 was expanded correlating with an increase in proliferating basal cells. Notably, p63 can transcriptionally repress the 14-3-3σ promoter, maintaining the proliferative capacity of keratinocyte SCs (Westfall *et al.*, 2003). Likewise, 14-3-3σ has been shown to promote the generation of transit-amplifying cells from basal keratinocyte SCs (Dellambra *et al.*, 2000; Pellegrini *et al.*, 2001), emphasising the delicate balance 14-3-3σ plays between proliferation and differentiation.

Further investigation into the abnormal IFE revealed basal cell proliferation was significantly higher during HF morphogenesis (P7) through to telogen of the adult cycle (P20). IFE thickness also followed a similar pattern being consistently thicker than wild-type IFE (Figure 5). Taken together with data showing an expansion of IFE basal markers, our data suggest *Sfn*$^{+/Er}$ mice are defective in the switch from proliferation to differentiation, resulting in an increased pool of proliferative transit-amplifying cells. Further support for this hypothesis is derived from a recent study on mice over-expressing the keratinocyte SC marker p63 (ΔNp63α) under the *Krt5* promoter (Romano *et al.*, 2010).

Yap1 has recently been shown to be a determinant of the proliferative capacity of epidermal SCs. We demonstrated increased nuclear Yap1 expression in the IFE of *Sfn*$^{+/Er}$ mice at P20 and detected increased total Yap1 protein by western blot at both ages, which correlated with a thickened, hyperproliferative IFE (Figure 5). Interestingly, smaller doublet protein bands were detected only in *Sfn*$^{+/Er}$ samples. These bands were consistent and appear to be specific to the *Sfn*$^{+/Er}$ disease phenotype. These unidentified bands might represent different Yap1 isoforms, indicating a more complex interaction than previously thought, possibly involving other molecular players and warrants further investigation. 14-3-3σ, α-catenin and Yap1 form a tripartite complex in the cytoplasm and function as negative upstream regulators of Yap1 (Schlegelmilch *et al.*, 2011; Silvis *et al.*, 2011). Expression of α-catenin was similar in *Sfn*$^{+/Er}$ IFE at both ages, indicating the increase in Yap1 was not due to loss of α-catenin. Our results complement previous gain- and loss-of-function studies demonstrating that disruption of 14-3-3σ (in this case a heterozygous dominant-negative mutation) leads to reduced cytoplasmic localisation and therefore increased nuclear Yap1 (Schlegelmilch *et al.*, 2011). Activated nuclear Yap1 has been shown to expand the epidermal SC compartment, increase epidermal proliferation at the expense of terminal differentiation and also lead to squamous cell carcinomas (SCC) (Zhang *et al.*, 2011; Schlegelmilch *et al.*, 2011; Silvis *et al.*, 2011). *Sfn*$^{+/Er}$ mice display enlarged epithelial appendages (HFs, SGs, nails), a hyperproliferative IFE, and are prone to SCC. Taken together, our results suggest these features of *Sfn*$^{+/Er}$ mice may be due in part to loss of regulation of Yap1.

Investigation into the quiescence of SCs within the HF bulge suggested the slowly cycling SCs (LRCs) were much more active in *Sfn*$^{+/Er}$ mice, as judged by a lack of label-retention after a 70 day BrdU chase (Figure 6). Given that HF bulge SC markers were present, appeared expanded and didn't contribute to the SGs or IFE in *Sfn*$^{+/Er}$ mice, we conclude the bulge cells have a cycling defect and proliferate more than normal. Although expression of 14-3-3σ within the K15-positive bulge is comparatively low (Figure S1), it is tempting to speculate mutant 14-3-3σ directly affects the proliferation of HF-SCs. Given the interaction with Yap1 and its regulation of epidermal SCs, it is possible a similar mechanism may exist within the HF bulge. It is also plausible that since 14-3-3σ is strongly expressed in keratin 6-positive companion layer cells surrounding the club hair (inner bulge cells), perturbations in this layer due to mutant 14-3-3σ can directly affect the quiescence of neighbouring HF-SCs (Hsu *et al.*, 2011).

In summary we have defined the expression profile of 14-3-3σ during HF development and investigated epithelial defects associated with a heterozygous dominant-negative mutation in 14-3-3σ. We have shown 14-3-3σ is critical for HF development, in particular formation of the hair shaft. Our results reinforce previous studies that 14-3-3σ acts as a growth suppressor in epithelial tissues, highlighted by perturbations in the homeostasis of SGs and the IFE of *Sfn*$^{+/Er}$ mice. We also highlighted a possible role for 14-3-3σ, either directly or indirectly, in maintenance of the HF bulge. Further investigation is required to elucidate the function of Yap1 in HF-SCs and whether a similar mechanism exists in the HF bulge, as has been shown for epithelial SCs.

Materials and Methods

Animals

Mice were obtained from Jackson Laboratories (mixed strain, C57BL/6J and CBA/CaGnLeJ; strain #000515). All experiments were repeated on at least three animals per genotype, unless stated and performed in accordance with the Animals (Scientific Procedures) Act UK 1986.

Histology, Oil Red O and Immunofluorescence

Backskin was fixed in 4% paraformaldehyde, wax processed, sectioned for immunofluorescence or stained with haematoxylin and eosin. Cryosections were stained in 0.5% Oil Red O in 100% isopropanol for 15 min and counterstained with haematoxylin. See supplemental methods for antibodies.

Scanning electron microscopy

Backskin was fixed in 2.5% glutaraldehyde/0.1 M sodium cacodylate, post-fixed in osmium tetroxide, washed in 0.1 M sodium cacodylate buffer, dehydrated, critical point dried, sputter-coated with gold and viewed in a Cambridge Stereoscan 360.

Proliferation assay

Mice were injected intraperitoneally, 100 μg/g body weight of BrdU (Amersham, UK) 4 hours prior to sacrifice. Processed backskin was immunostained with anti-BrdU. Consecutive microscope images (x20 fields) were taken and a proliferation index of basal BrdU IFE cells was calculated. 700-900 basal IFE cells were counted per animal (n=3 per genotype).

BrdU label-retaining assay

P10 mice were injected intraperitoneally, 50 g/g body weight of BrdU every 12 hours for 48 hours and sacrificed 70 days later (n=5 per genotype). Mice were taken at P13 to assess for BrdU labelling efficiency, using immunofluorescence. Backskin was processed and immunostained with antibodies against BrdU and K15.

Real-time qPCR

Total RNA was extracted using RNeasy kit (Qiagen, UK) from full thickness skin (pooled samples, wild-type: n=3, $Sfn^{+/Er}$: n=7), quantified and reverse transcribed to cDNA. qPCR was performed as per manufacturer's instructions on a StepOne Plus machine using SYBR Green master mix (Life Technologies, UK) and analysed using ΔΔ-Ct method, normalised to β-actin. See supplemental for primers.

Western Blot

Protein lysates were prepared from P7 and P20 backskin, resolved on 9% SDS-PAGE gels, transferred to nitrocellulose membranes (Bio-Rad, UK) and immunoblotted using anti-Yap1 (1:500) (Cell Signalling) and anti-β-actin (1:20,000) (Sigma-Aldrich, UK). Immune complexes were detected using HRP-conjugated secondary antibodies (1:3000) and SuperSignal West Pico chemiluminescence (Thermo Scientific, UK).

Supplementary Material

Refer to Web version on PubMed Central for supplementary material.

Acknowledgments

We thank the Wellcome Trust (082868) for funding.

Abbreviations

HF	hair follicle
SC	stem cell

IFE	inter-follicular epidermis
SG	sebaceous gland
Sfn	stratifin

References

Aitken A. 14-3-3 proteins: a historic overview. Semin Cancer Biol. 2006; 16:162–72. [PubMed: 16678438]

Blanpain C, Fuchs E. Epidermal stem cells of the skin. Annu Rev Cell Dev Biol. 2006; 22:339–73. [PubMed: 16824012]

Cai J, Lee J, Kopan R, et al. Genetic interplays between Msx2 and Foxn1 are required for Notch1 expression and hair shaft differentiation. Dev Biol. 2009; 326:420–30. [PubMed: 19103190]

Camargo FD, Gokhale S, Johnnidis JB, et al. YAP1 increases organ size and expands undifferentiated progenitor cells. Curr Biol. 2007; 17:2054–60. [PubMed: 17980593]

Cotsarelis G, Sun TT, Lavker RM. Label-retaining cells reside in the bulge area of pilosebaceous unit: implications for follicular stem cells, hair cycle, and skin carcinogenesis. Cell. 1990; 61:1329–37. [PubMed: 2364430]

Dellambra E, Golisano O, Bondanza S, et al. Downregulation of 14-3-3sigma prevents clonal evolution and leads to immortalization of primary human keratinocytes. J Cell Biol. 2000; 149:1117–30. [PubMed: 10831615]

Fisher C, Jones A, Roop DR. Abnormal expression and processing of keratins in pupoid fetus (pf/pf) and repeated epilation (Er/Er) mutant mice. J Cell Biol. 1987; 105:1807–19. [PubMed: 2444602]

Ghazizadeh S, Taichman LB. Multiple classes of stem cells in cutaneous epithelium: a lineage analysis of adult mouse skin. EMBO J. 2001; 20:1215–22. [PubMed: 11250888]

Guenet JL, Salzgeber B, Tassin MT. Repeated epilation: a genetic epidermal syndrome in mice. J Hered. 1979; 70:90–4. [PubMed: 479550]

Hardy MH. The secret life of the hair follicle. Trends Genet. 1992; 8:55–61. [PubMed: 1566372]

Herron BJ, Liddell RA, Parker A, et al. A mutation in stratifin is responsible for the repeated epilation (Er) phenotype in mice. Nat Genet. 2005; 37:1210–2. [PubMed: 16200063]

Higgins CA, Westgate GE, Jahoda CA. From telogen to exogen: mechanisms underlying formation and subsequent loss of the hair club fiber. J Invest Dermatol. 2009; 129:2100–8. [PubMed: 19340011]

Horsley V, O'Carroll D, Tooze R, et al. Blimp1 defines a progenitor population that governs cellular input to the sebaceous gland. Cell. 2006; 126:597–609. [PubMed: 16901790]

Hsu YC, Pasolli HA, Fuchs E. Dynamics between stem cells, niche, and progeny in the hair follicle. Cell. 2011; 144:92–105. [PubMed: 21215372]

Ito M, Liu Y, Yang Z, et al. Stem cells in the hair follicle bulge contribute to wound repair but not to homeostasis of the epidermis. Nat Med. 2005; 11:1351–4. [PubMed: 16288281]

Jaks V, Barker N, Kasper M, et al. Lgr5 marks cycling, yet long-lived, hair follicle stem cells. Nat Genet. 2008; 40:1291–9. [PubMed: 18849992]

Jaks V, Kasper M, Toftgard R. The hair follicle-a stem cell zoo. Exp Cell Res. 2010; 316:1422–8. [PubMed: 20338163]

Jensen KB, Collins CA, Nascimento E, et al. Lrig1 expression defines a distinct multipotent stem cell population in mammalian epidermis. Cell Stem Cell. 2009; 4:427–39. [PubMed: 19427292]

Kiso M, Tanaka S, Saba R, et al. The disruption of Sox21-mediated hair shaft cuticle differentiation causes cyclic alopecia in mice. Proc Natl Acad Sci U S A. 2009; 106:9292–7. [PubMed: 19470461]

Li Q, Lu Q, Estepa G, et al. Identification of 14-3-3sigma mutation causing cutaneous abnormality in repeated-epilation mutant mouse. Proc Natl Acad Sci U S A. 2005; 102:15977–82. [PubMed: 16239341]

Europe PMC Funders Author Manuscripts

Ma L, Liu J, Wu T, et al. 'Cyclic alopecia' in Msx2 mutants: defects in hair cycling and hair shaft differentiation. Development. 2003; 130:379–89. [PubMed: 12466204]

McGowan KM, Tong X, Colucci-Guyon E, et al. Keratin 17 null mice exhibit age- and strain-dependent alopecia. Genes Dev. 2002; 16:1412–22. [PubMed: 12050118]

Medina A, Ghaffari A, Kilani RT, et al. The role of stratifin in fibroblast-keratinocyte interaction. Mol Cell Biochem. 2007; 305:255–64. [PubMed: 17646930]

Millar SE. Molecular mechanisms regulating hair follicle development. J Invest Dermatol. 2002; 118:216–25. [PubMed: 11841536]

Milner Y, Sudnik J, Filippi M, et al. Exogen, shedding phase of the hair growth cycle: characterization of a mouse model. J Invest Dermatol. 2002; 119:639–44. [PubMed: 12230507]

Morrison DK. The 14-3-3 proteins: integrators of diverse signaling cues that impact cell fate and cancer development. Trends Cell Biol. 2009; 19:16–23. [PubMed: 19027299]

Nijhof JG, Braun KM, Giangreco A, et al. The cell-surface marker MTS24 identifies a novel population of follicular keratinocytes with characteristics of progenitor cells. Development. 2006; 133:3027–37. [PubMed: 16818453]

Owens P, Bazzi H, Engelking E, et al. Smad4-dependent desmoglein-4 expression contributes to hair follicle integrity. Dev Biol. 2008; 322:156–66. [PubMed: 18692037]

Pellegrini G, Dellambra E, Golisano O, et al. p63 identifies keratinocyte stem cells. Proc Natl Acad Sci U S A. 2001; 98:3156–61. [PubMed: 11248048]

Romano RA, Smalley K, Liu S, et al. Abnormal hair follicle development and altered cell fate of follicular keratinocytes in transgenic mice expressing DeltaNp63alpha. Development. 2010; 137:1431–9. [PubMed: 20335364]

Schlegelmilch K, Mohseni M, Kirak O, et al. Yap1 acts downstream of alpha-catenin to control epidermal proliferation. Cell. 2011; 144:782–95. [PubMed: 21376238]

Shimomura Y, Christiano AM. Biology and genetics of hair. Annu Rev Genomics Hum Genet. 2010; 11:109–32. [PubMed: 20590427]

Silvis MR, Kreger BT, Lien WH, et al. alpha-catenin is a tumor suppressor that controls cell accumulation by regulating the localization and activity of the transcriptional coactivator Yap1. Sci Signal. 2011; 4:ra33. [PubMed: 21610251]

Snippert HJ, Haegebarth A, Kasper M, et al. Lgr6 marks stem cells in the hair follicle that generate all cell lineages of the skin. Science. 2010; 327:1385–9. [PubMed: 20223988]

Stenn K. Exogen is an active, separately controlled phase of the hair growth cycle. J Am Acad Dermatol. 2005; 52:374–5. [PubMed: 15692497]

Stenn KS, Paus R. Controls of hair follicle cycling. Physiol Rev. 2001; 81:449–94. [PubMed: 11152763]

Taylor G, Lehrer MS, Jensen PJ, et al. Involvement of follicular stem cells in forming not only the follicle but also the epidermis. Cell. 2000; 102:451–61. [PubMed: 10966107]

Watt FM, Hogan BL. Out of Eden: stem cells and their niches. Science. 2000; 287:1427–30. [PubMed: 10688781]

Westfall MD, Mays DJ, Sniezek JC, et al. The Delta Np63 alpha phosphoprotein binds the p21 and 14-3-3 sigma promoters in vivo and has transcriptional repressor activity that is reduced by Hay-Wells syndrome-derived mutations. Mol Cell Biol. 2003; 23:2264–76. [PubMed: 12640112]

Xin Y, Lu Q, Li Q. 14-3-3sigma controls corneal epithelial cell proliferation and differentiation through the Notch signaling pathway. Biochem Biophys Res Commun. 2010a; 392:593–8. [PubMed: 20100467]

Xin Y, Lu Q, Li Q. 14-3-3sigma is required for club hair retention. J Invest Dermatol. 2010b; 130:1934–6. [PubMed: 20237493]

Zhang H, Pasolli HA, Fuchs E. Yes-associated protein (YAP) transcriptional coactivator functions in balancing growth and differentiation in skin. Proc Natl Acad Sci U S A. 2011; 108:2270–5. [PubMed: 21262812]

Europe PMC Funders Author Manuscripts

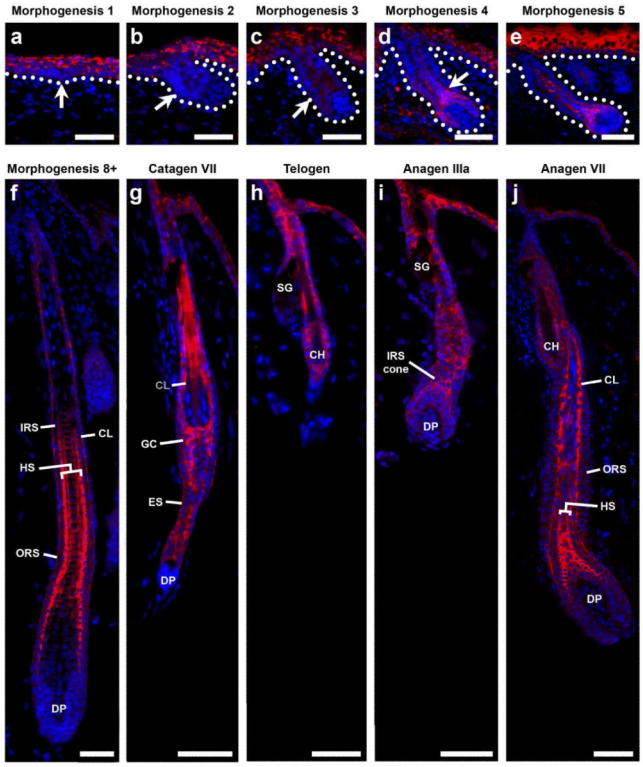

Figure 1. 14-3-3σ expression during hair morphogenesis and cycling

Developing placodes (a), hair germs (b) and hair pegs (c) were devoid of 14-3-3σ (arrows) with expression first seen in the inner root sheath (IRS) cone (d, arrow) and becoming restricted to the HF bulb (e). (f) 14-3-3σ was restricted to the hair shaft (HS), companion layer (CL) and outer root sheath (ORS) in stage 8+ HFs. (g) During catagen, 14-3-3σ was expressed in the CL, germ capsule (GC) and epithelial strand (ES). (h) 14-3-3σ was also expressed in cells surrounding the club hair (CH). In anagen, 14-3-3σ was expressed in the IRS cone (i) subsequently expanding to the CL and HS, with low expression in the ORS (j). Scale bars: 50 μm.

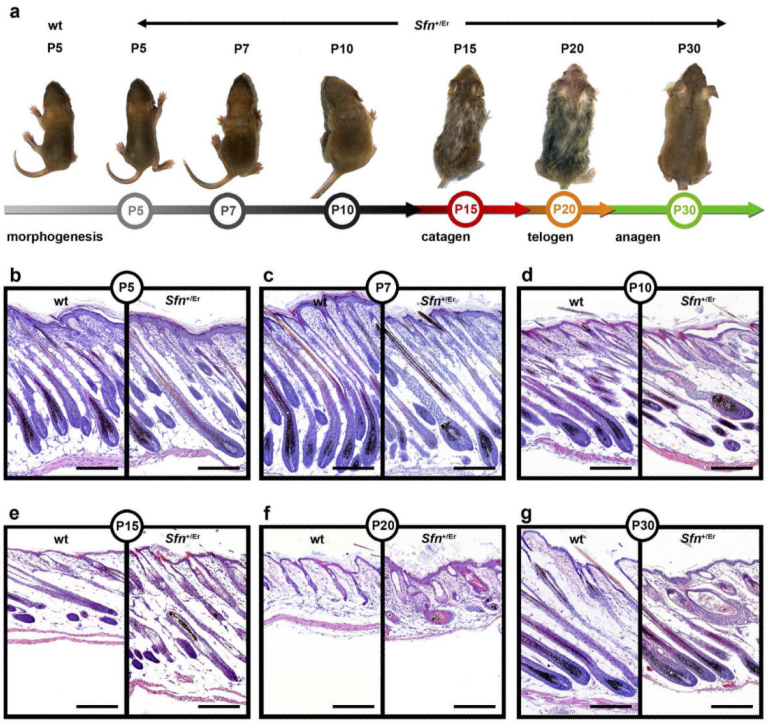

Figure 2. *Sfn*$^{+/Er}$ mice develop cyclic alopecia

(a) Alopecia was first apparent on head and neck regions at P7. Hair loss advanced with age to affect lower dorsal regions by P15. The majority of pelage was lost by telogen (P20). Pelage hair was restored in the subsequent anagen (P30). (b, c) P5 histology was normal but by P7 affected HFs were twisted with abnormal HF bulbs. (d) Problems with hair shaft production were apparent by P10. (e) Many HFs were missing a hair shaft by catagen, this becoming most obvious at telogen (f). Hair was restored during the next anagen but HF abnormalities manifested again by P30 (g). Scale bars: 200 μm.

Europe PMC Funders Author Manuscripts

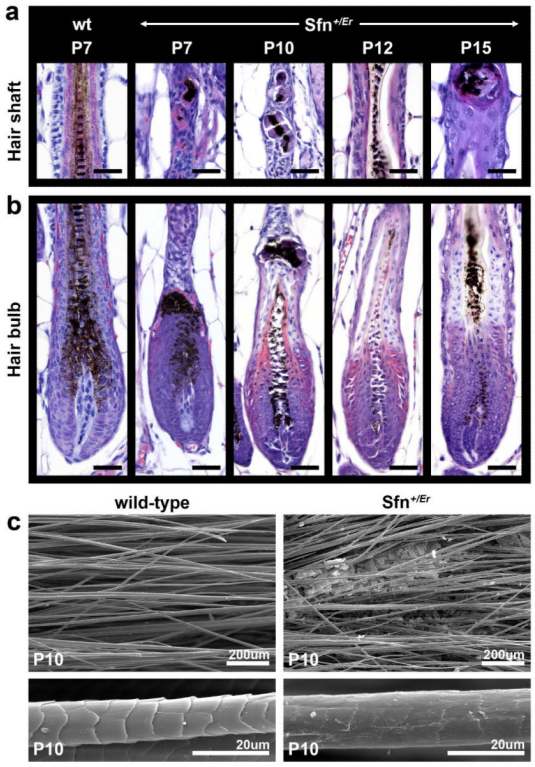

Figure 3. Abnormalities in hair shaft differentiation results in hair loss

Histology of dystrophic hair follicles showed abnormalities in the companion layer (CL), inner root sheath (IRS) and hair shaft (HS). In severely affected follicles, CL, IRS and HS layers formed keratinous blebs full of melanin granules (P7, P10, P15 in a). Less affected follicles formed a HS but abnormalities in septation and HS thickness were seen along its length (P12 in a). The hair bulbs of affected follicles showed abnormalities in the precortex region with HS and IRS layers showing irregular cell morphology, cell-cell spaces and highly eosinophilic (b). SEM analysis demonstrated a sparse pelage coat at P10 and abnormal cuticle formation in *Sfn*$^{+/Er}$ mice (c). Scale bars: a,b, 50 μm).

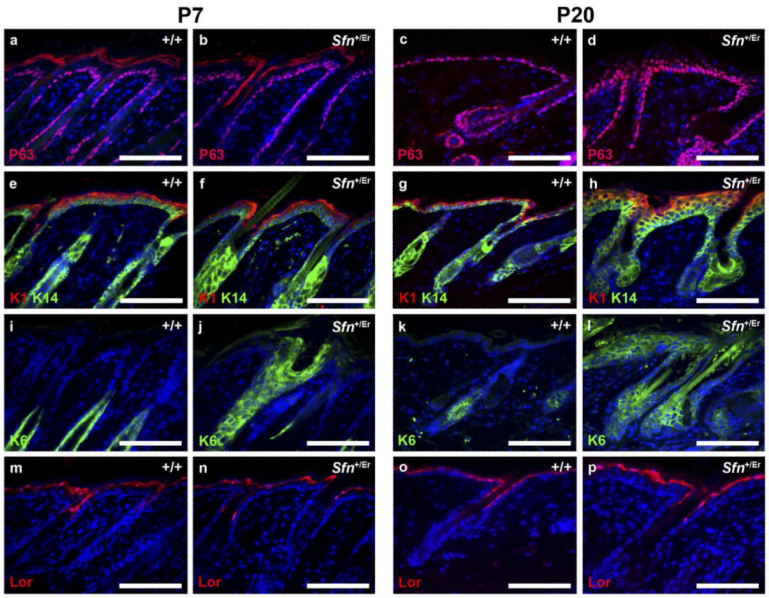

Figure 4. Analysis of the interfollicular epidermis

Immunofluoresence staining of molecular markers in wild-type and *Sfn*$^{+/Er}$ skin at P7 (morphogenesis) and P20 (telogen). P63 (a-d), keratin 14 (K14; green) with keratin 1 (K1; red) (e-h), keratin 6 (K6) (i-l) all showed slight expansion in *Sfn*$^{+/Er}$ skin at P7, but was massively increased by P20. Loricrin (Lor) expression was comparable to wild-type skin at both ages (q-t). Fluorescent colour reflects the secondary antibody used. Scale bars: 100 μm (e-l), 50 μm (m-x).

Europe PMC Funders Author Manuscripts

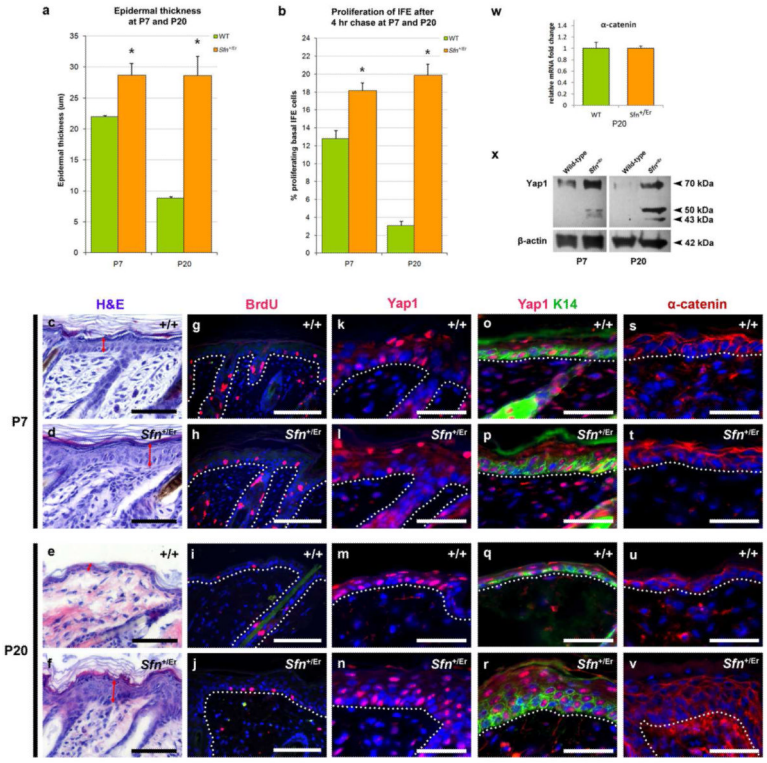

Figure 5. *Sfn*$^{+/Er}$ IFE is hyperproliferative

(a) Epidermal thickness at P7 and P20 was measured and compared, as indicated in H&E sections (c-f). (b) The proliferation index of the IFE was measured by BrdU incorporation (g-j) and compared at the same ages. Immunofluorescence for Yap1 (k-n) and Yap1/K14 (o-r) showed nuclear Yap1 was expressed throughout the IFE at both ages. (k,l) Nuclear Yap1 expression was similar at P7. (m,n) At P20, more cells are positive for nuclear Yap1 in *Sfn*$^{+/Er}$ skin. (s-v) α-catenin expression was comparable at both ages, and complimented qPCR data at P20 (w). (x) Western blot confirmed elevated Yap1 protein levels in *Sfn*$^{+/Er}$ lysates at both ages. Scale bars: e-l, 100 μm, m-x, 50 μm, mean +/-SEM, n=3 per genotype, p=0.05.

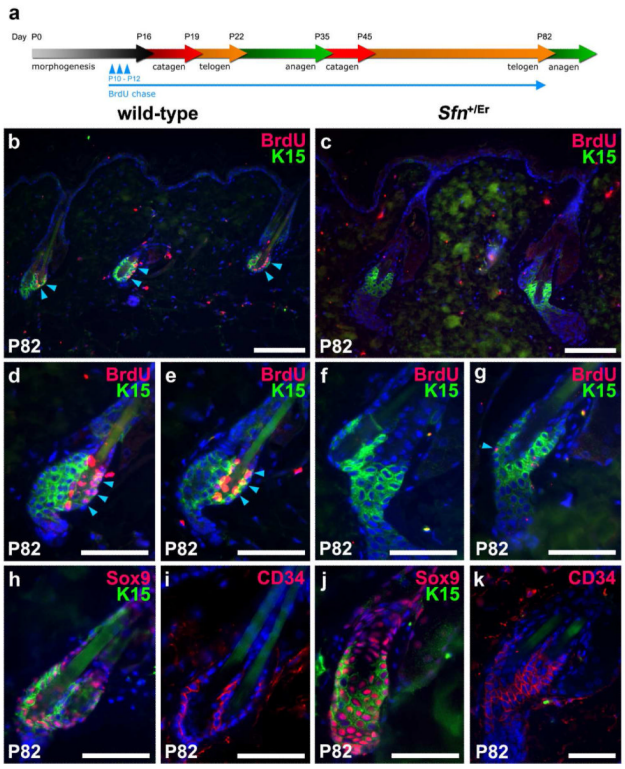

Figure 6. Depletion of label-retaining cells in the hair follicle bulge

(a) Mice injected with BrdU every 12 hours from P10 - P12 were chased for 70 days until the second telogen. Dual-labelling with K15 and BrdU enabled label retaining cells (LRCs) to be identified within the HF bulge. Wild-type HFs displayed numerous K15-positive LRCs (b,d,e; arrowheads) compared to a complete lack of LRCs in *Sfn*$^{+/Er}$ HFs (c,f,g). Occasionally a few grains of diluted BrdU label were seen in *Sfn*$^{+/Er}$ K15-positive cells (g; arrowhead). (h-k) Sox9 and CD34 markers were present and appeared expanded in the HF bulge. Scale bars: 100 μm.

Europe PMC Funders Author Manuscripts